Article citation info:
Zhang J, Li Y, Hao X, Ma J, Xue H, Han C, Wu J, Dang X. Fiber optic cable performance monitoring and optimization research based on multiple environmental parameters. Diagnostyka. 2025;26(3):2025314. https://doi.org/10.29354/diag/209048.

DIAGNOSTYKA, 2025, Vol. 26, No. 3

e-ISSN 2449-5220
DOI: 10.29354/diag/209048

FIBER OPTIC CABLE PERFORMANCE MONITORING AND OPTIMIZATION RESEARCH BASED ON MULTIPLE ENVIRONMENTAL PARAMETERS

Jianliang ZHANG *, **Yang LI**, **Xiaowei HAO**, **Junwei MA**, **Honglin XUE**, **Chao HAN**, **Jian WU**, **Xiaoyan DANG**

State Grid Information & Telecommunication CO. of Shanxi Electric Power Company, Taiyuan 030021, China
* Corresponding author, e-mail: sxdlzjl@163.com

Abstract

One essential requirement for guaranteeing the secure and reliable functioning of the electricity system is the regular functioning of fiber optic cable connections. To timely grasp the real-time operation status of the fiber optic lines, the study proposes a fiber optic cable performance monitoring method based on a variety of environmental parameters. This method involves the measurement of optical fiber-type light intensity of the fiber optic cable line, which is used for safety monitoring, monitoring and analysis of fiber optic cable lines, and the design of a fiber optic cable outer layer broken strands of high precision monitoring method, which combines fiber grating sensing. To optimize the monitoring method of fiber optic cable performance, the study was based on fiber optic coupling efficiency and numerical aperture for parametric measurement loss analysis. The results indicated that the signal-to-noise ratio of the fiber optic sensor can be up to 152 and 157 dB, and the response frequency can be up to 6233 and 6315 times/s. Adjusting the bending radius can effectively control the degree of loss of the optical fiber. Compared with 1550 nm, the loss of single-mode fiber G.6521 at 1310 nm wavelength was much lower than that of multi-mode fiber. It can be observed that the monitoring method proposed by the study is an effective means of monitoring the defects of optical cable operation, providing reliable protection for the fault monitoring of the outer layer of the cable in remote areas, improving the operational efficiency of the power system, and effectively monitoring the performance of the cable. This is crucial to implementing the management of the optical cable's safety performance assessment since it establishes the framework for it.

Keywords: fiber optic sensing network, fiber optic cable outer layer broken strands, integrated circuit bus, high precision monitoring, light intensity

1. INTRODUCTION

China's fiber optic (FO) transmission lines are widely employed in many different industries. One of the main research hotspots in transmission line monitoring is the pursuit of efficient and accurate data monitoring to permit prompt line warning. Among them, the monitoring of fiber optic cable (FOC) outer layer broken strands faults is the main cause of transmission accidents. Therefore, in order to reduce the economic loss caused by the high incidence of faults, as well as to eliminate the hidden dangers and extend the service life of FOC, a variety of monitoring methods have been proposed at home and abroad (1,2). FO hydrophones, which are simple devices for detecting hydroacoustic waves, have advanced quickly in recent years thanks to their fiber optic sensing (FOS) and communication technologies. Deploying deep learning models on mobile terminals aboard marine survey vessels is challenging due to their vast number of parameters. To improve performance, Lyu C. et al. designed the deep lightweight attention residual network (DLA-ResNet), which adds convolutional block attention modules and depth separable convolution to ResNet18. The outcomes revealed that the enhanced DLA-ResNet's accuracy increased by approximately 2.04% and its size decreased by 85.67%. The average recognition rate of eight underwater FOS signals reached 96.50%, and the size of the model was only 6.12MB, which took only 27.90ms, meeting the reliability and validity requirements (3). To assess the efficacy of FO monitoring in active sinkholes, Gutierrez F. et al. compared vertical displacement data acquired with a high degree of precision with stresses recorded by two different types of fiber cable, demonstrating a strong spatial and temporal correlation. The findings indicated that testing different kinds of sinkholes with more confined deformation zones and higher settlement

Received 2025-05-10; Accepted 2025-08-06; Available online 2025-09-10

rates, as well as enhancing the monitoring system, could yield better outcomes (4). In a long-distance HVDC operating environment, Liu Z. et al. conducted a partial discharge FO ultrasonic detection system with the goal of enhancing the safety and effectiveness of partial discharge detection in high voltage direct current (HVDC) cable systems. The measurement findings confirmed the partial discharge FO detection system's intrinsic safety dependability as well as the partial discharge sites' detection efficiency in HVDC cable systems (5). A technique for employing FO to track the cutting depth during electrochemical machining was presented by Zhou F. et al. The findings demonstrated that there was a discrepancy of less than 4% between the final machining depth determined by the profilometer and the sensor, which may be explained by the electrolyte's changing refractive index during the machining process (6).

Distributed strain measurements from FOS can improve the capabilities of laboratory testing and structural health monitoring (SHM). Liu H. et al. investigated the effectiveness of using optical frequency domain reflection method (OFDR) strain sensing to assess concrete cracking behavior and reinforcement deformation. To precisely quantify fracture width, the study used two types of fiber cables: one with a higher sensitivity and the other with a lower sensitivity but a better survival. The study's findings showed that widespread microcrack detection and accurate crack width determination can be achieved by combining OFDR strain sensing with a novel data processing technique (7). For cable lines to operate safely and steadily, partial discharges in cable terminations must be observed. Hao Y. et al. developed a partial discharge Mach Zehnder interferometer (MZI) detection system for crosslinked polyethylene (PE) cable termination. The findings demonstrated that, for a cylindrical air-gap defect sample with a base radius of 1.5 mm and a height of 3 mm, the fiber-optic MZI could detect partial discharges of 196 pC (8). A distributed FO monitoring methodology was introduced by Hou G. Y. as a means of estimating the continuous deformation of concrete beams. With a maximum inaccuracy of only 2.7%, the results showed that the trained neural network's deformation values were extremely similar to those of the total station. The findings of the simulation were deemed reliable as the goodness of fit R-2, as determined by linear regression analysis, was higher than 0.98 (9). Zhang S. et al. looked into the efficacy of OFDR when applied with various kinds of fiber cable in identifying large strain steel deformations and cracks in concrete. The findings showed that OFDR was able to identify strain localization suggestive of concrete cracking, continuing steel deformation, and bond stresses across the post-yield range (10). A fiber Bragg grating temperature sensing demodulation system based on optical power detection was proposed by Huang S. According to the findings, over a temperature range of 10 to 85 degrees centigrade, the linearity coefficients R-squared between the optical power and the sampling voltage were 0.99908 and 0.99893, respectively (11).

In conclusion, researchers have conducted comprehensive studies on FO data identification, performance monitoring, and optimization of monitoring methods. However, the monitoring accuracy and sensitivity of the aforementioned FOC monitoring methods are limited, primarily due to the susceptibility of the methods to noise interference, which compromises the signal-to-noise ratio (SNR) of the monitored signals, such as the temperature of the FOC, and the response frequency of the sensor. Therefore, the study proposes a FOC performance monitoring method based on a variety of environmental parameters. The method is innovative to the fiber grating (FG) sensing based on the FOC outer layer broken strands for high-precision monitoring research. A design parameter measurement loss analysis method is employed to calculate the FO coupling efficiency and numerical aperture, thereby enabling the detection of the performance of FOCs and the assurance of their normal operation. This method also provides a technical basis for the optimization of FO performance monitoring.

The first part of this research describes the research background, research significance and existing research prospects of FO communication and performance monitoring. The second part focuses on the process of the FOC performance monitoring method based on multiple environmental parameters, which is also the focus and innovation point of this research. The third section describes the experimental validation based on the algorithm designed in the second section and analyzes the results of the experimental data. The fourth part concludes the experimental results and describes the shortcomings of the design and the direction for further development.

2. METHODS AND MATERIALS

A two-dimensional signal model is constructed based on the temperature data of the outer layer of the FOC. This is used for high precision monitoring of the outer strand break of the FOC. In order to optimize the testing method of FOC performance, the study calculates the corresponding parameters through the measurement of fiber connection loss, optical attenuator parameters, as well as fiber bending loss and multi-mode optical patchcord insertion loss. Furthermore, the study investigates the methods to reduce the fiber loss.

2.1. High precision monitoring method for fiber optic cable outer layer broken strands based on fiber grating sensing

The FOC is mostly divided into two sections: the core and the polymer sheath. PE has become the mainstream FOC sheath material because of its good chemical stability, superior dielectric properties and many other characteristics (12,13). To effectively monitor the FOC outer sheath breakage and to effectively realize the sensitivity of the monitoring process, the study is conducted to monitor the accuracy of the FOC outer layer broken strands. According to the temperature data of FOC outer layer, the study constructs the corresponding two-dimensional signal model, in which the wavelet denoising algorithm is introduced and applied to the monitoring data acquisition. In order to determine the temperature amplitude and fiber location, the study employs the optical time-domain reflection method (14,15).

Broken strands will not only negatively affect the working of the circuit, but will also shorten the life of the wire considerably. Each broken strand in a wire indicates that its internal structure has been damaged. This damage may gradually spread over the course of use, which in turn leads to damage to the overall structure of the wire, and the wire's lifespan will inevitably be compromised. Determine whether the FOC is completely out of service by performing transmit optical power detection at both ends of the optical path. If the FOC is completely interrupted, select several access points in the middle of the optical path for testing. The approximate location of the break point is determined by the bisection method. A detailed test is performed near the break point to determine the exact location of the break point of the FOC. Failure cause determination: Check whether the environment near the break point has obvious signs of external damage. Examine the section with an optical magnifying glass to determine whether it is aged and brittle. Open the hand hole and check whether there is any connector problem or flooding condition. Determine the cause of interruption of the FOC based on the state of the breakpoint. The condition of FOC breakage is monitored according to the temperature change. To obtain temperature data from the outer layer of the FOC, it is necessary to install the corresponding FO temperature sensor on the cable itself. Fig. 1 displays the FO temperature sensor. In Fig. 1, the commands sent by the research system are the main processor used, which is the main control component of the sensor that operates through the IIC bus and processes the feedback data. During the application of the sensor, the device is able to effectively control the pulse drive circuitry by regulating the optical pulse signal from the laser. To ensure that the temperature of the laser is stabilized and that the optical pulse signal is able to change wavelength as the temperature of the outer layer of the FOC changes, it is necessary to utilize the change in temperature to achieve line control. FG is a type of diffraction grating created by a passive filter mechanism that modifies the refractive index of the fiber core axially and periodically. Using the fiber material's photosensitivity is the primary method of FG synthesis. By using UV to write the coherent field pattern of incident light into the fiber core, a phase grating in permanent space is formed, which is a periodic change in the refractive index along the axial direction of the core inside the core (16,17).

To increase the accuracy of detection and decrease errors resulting from other causes, the study thoroughly examines the wavelength drift induced by temperature and strain, respectively. The amount of visible light received per unit area is known as light intensity. Which results from photoionization-induced photoelectron emission, or the photoelectric effect. Under the action of light can make electrons escape from the surface of the object is called "external photoelectric effect" or photoelectric emission.

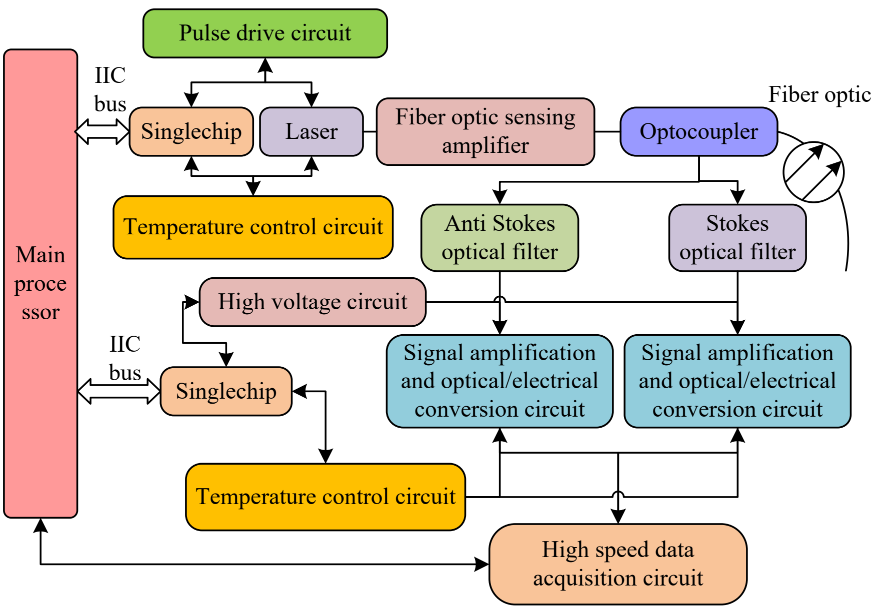

Fig. 1. Fibre optic temperature sensor system specific structure

Equation (1) expresses the photoelectric effect from the outside.

$$hv = E_k + W \quad (1)$$

In Equation (1), E_k denotes the electron kinetic energy and v denotes the frequency of the incident light. W denotes the electron spillover energy and h denotes Planck's constant. The external photoelectric effect is shown in Fig. 2.

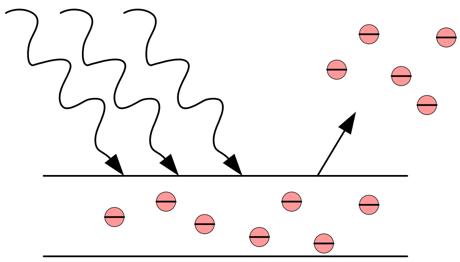

Fig. 2. Principle of external photoelectric effect

Light intensity refers to the luminous flux of visible light received per unit area, which is referred to as illuminance (Lux or lx). It is calculated as in Equation (2).

$$E_T = \frac{d\Phi}{dS} \quad (2)$$

In Equation (2), E_T denotes luminous flux irradiated per unit area. Φ denotes luminous flux. S denotes illuminated area (18). It is assumed that the relationship between the light intensity value and the current value within the error tolerance can be expressed as in Equation (3).

$$E_L = kI_L \quad (3)$$

In Equation (3), E_L denotes the light intensity. I_L denotes the current corresponding to the solar panel circuit. k denotes the current coefficient, which can be confirmed by comparison test. The studied fiber-optic Light intensity sensing and monitoring device is based on fiber-optic grating and cantilever beam, and the force analysis of the cantilever beam is shown in Fig. 3.

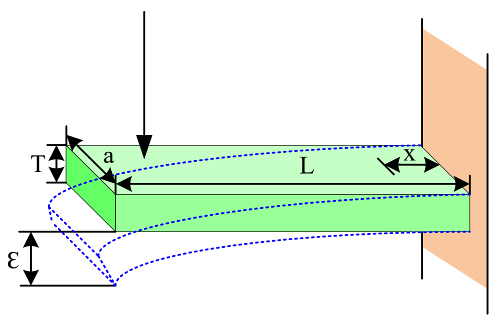

Fig. 3. Force analysis of cantilever beams

In Fig. 3, the cantilever beam sensor is a sensing and measuring device based on the cantilever beam deformation principle. It consists of one or more cantilever beams, each of which has a sensor mounted on it. When an object is placed on the cantilever beam, the resulting pressure causes the cantilever beam to deflect, which in turn applies pressure to the sensor and generates a specific electrical signal. The cantilever beam structure is one of the important devices for light intensity sensors. It is studied to use its strain to move the wavelength of a FG stress gauge affixed to it to accurately reflect the light intensity. M denotes the cantilever beam bending moment. The strain of the cantilever beam used in the study is within its elastic range and can be approximated as a line during the calculation. I denotes the cross-sectional moment of inertia of the cantilever beam structure. The approximate differential equation of the deflection curve is expressed as in Equation (4).

$$\begin{cases} M(x) = F(L-x) \\ E_Y I \rho(x) = M(x) \end{cases} \quad (4)$$

In Equation (4), E_Y denotes the Young's modulus of the cantilever beam material. By combining the radius of curvature $\rho(x) = \frac{d^2\omega}{dx^2}$ with Equation (4), the result is obtained as in Equation (5).

$$EI\frac{d^2\omega}{dx^2} = F(L-x) \quad (5)$$

Integrating Equation (5) twice yields Equation (6).

$$EI\omega = \frac{1}{6}F(L-x)^3 + Ax + B \quad (6)$$

The boundary conditions are utilized to obtain the variables as in Equation (7).

$$\begin{cases} A = \frac{1}{2}FL^2 \\ B = -\frac{1}{6}FL^3 \end{cases} \quad (7)$$

The winding degree equation of the cantilever beam is found as in Equation (8).

$$\omega = \frac{F}{6EI}(3Lx^2 - x^3) \quad (8)$$

The positive stress σ at any point in the cantilever beam cross-section is obtained as in Equation (9).

$$\sigma = \frac{M*y}{I} \quad (9)$$

In Equation (9), y denotes the distance from the calculation point to the neutral axis. σ denotes the positive stress. That is, in order to resist the stresses generated by deformation, the moment of inertia of a rectangular cantilever beam section can be obtained by analyzing a quantity that reflects the bending characteristics of the section, referred to as the moment of inertia. The axial moment of inertia of the cross-section with respect to an axis is equal to the integral of the square of the distance of each micro-area of the cross-section multiplied by the distance of the micro-area to the axis over the whole cross-section, which is calculated as in Equation (10).

$$\begin{cases} y = \dfrac{T}{2} \\ I = \dfrac{aT^3}{12} \end{cases} \quad (10)$$

Combined with the defining equation $\varepsilon = \dfrac{\sigma}{E}$ of strain, the joint Equation (4), (10) can get the strain at any point. Specific calculations are shown in Equation (11).

$$\varepsilon = \frac{6F(L-x)}{EaT^2} \quad (11)$$

Therefore, the absolute value of the strain on the compression surface can be obtained as a negative correlation.

2.2. Parametric measurement loss analysis based on fiber optic coupling efficiency and numerical aperture

In the above according to the temperature and light intensity to achieve the FOC line sensing detection, the need to achieve the measurement and analysis of FO loss, in order to optimize the FO loss detection. The study of FO loss type and related parameters has a very important significance in the practical application of FO. The FO coupling efficiency, NA size is an important research object in optical signal transmission and sensing technology. Absorption loss, insertion loss and bending loss of FO are also parameters that need to be monitored in FO cabling project (19). Therefore, in order to optimize the detection method of FOC performance, the study calculates the corresponding parameters and researches the methods to reduce FO loss through the measurement of fiber connection loss, optical attenuator parameters as well as fiber bending loss and multi-mode optical patch cord insertion loss.

FO coupling, which is the process of coupling light energy from a light source into a FO for transmission, is a crucial component of FO transmission and sensor technologies (20). The study measurements analyze the coupling of single-mode and multi-mode fibers and the optical path setup for FO coupling measurements is shown in Fig. 4.The NA of an FO is the parameter difference between the diameter of the center core of the FO transmission center and the refractive index of the cladding. It is an important index of FO transmission, which is directly related to FO transmission performance, optical signal transmission quality and other aspects. It characterizes the optical signal reception ability and transmission performance of the FO transmission center core. Specifically, the size of NA directly affects the optical signal loss in the FO, the transmission distance, and the bandwidth of the FO and other properties. In the light transmission process, the approximate radius of the circular spot is calculated as in Equation (12).

$$R = |R_1 - R_2| \quad (12)$$

L denotes the distance of the obtained fiber output from the face. The study uses a power meter that is at the center of the circular spot to measure the corresponding power, which is indicated by a micrometer filament scale. P_1 is the power at the current moment and P_2 is the boundary power. R_1 denotes the pan-table scale at the current moment. When $P_2 = 0.1P_1$, R_2 denotes the current moment scale after the power meter is moved. NA is calculated as in Equation (13).

$$NA = \mathrm{Sin}[\arctan(|R1 - R2|/L)] \quad (13)$$

The study uses an optical transmitter for testing and a small variable attenuator and the testing method is shear. To balance the mode distribution, the study uses a column mode scrambler and then the specified optical power is obtained. Finally, in order to obtain the output optical power, the small variable attenuator is connected to the circuit. The specific test flow is shown in Fig. 5.

Fiber loss is the attenuation per unit length of the fiber. The loss calculation formula is shown in Equation (14).

$$\alpha(\lambda) = 10 1\mathrm{g}\frac{P(Z_L)}{P_0} \quad (14)$$

In Equation (14), $P(Z_L)$ denotes the optical power at axial distance $Z = L$. $\alpha(\lambda)$ denotes the attenuation coefficient, which is located at wavelength λ. $P(0)$ denotes the optical power at axial distance $Z = 0$.

Bending loss is one of the most significant reducible losses in FO cabling, and a fiber wrap scrambler is a component that enables strong coupling of strongly geometrically perturbed modes. This component provides mode distributions that are independent of the characteristics of the light source. Using this component to simulate fiber bending, the bending loss can be calculated using the formula (15).

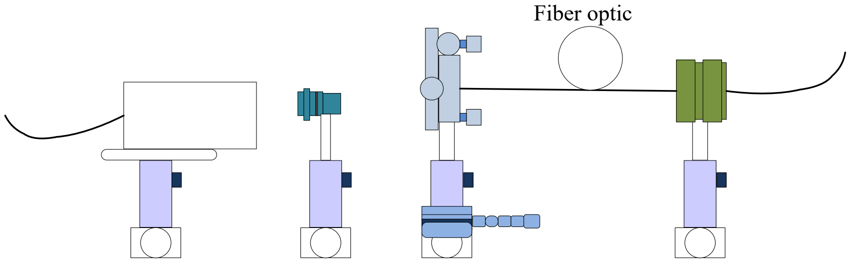

Fig. 4. Fiber optic coupling measurement diagram

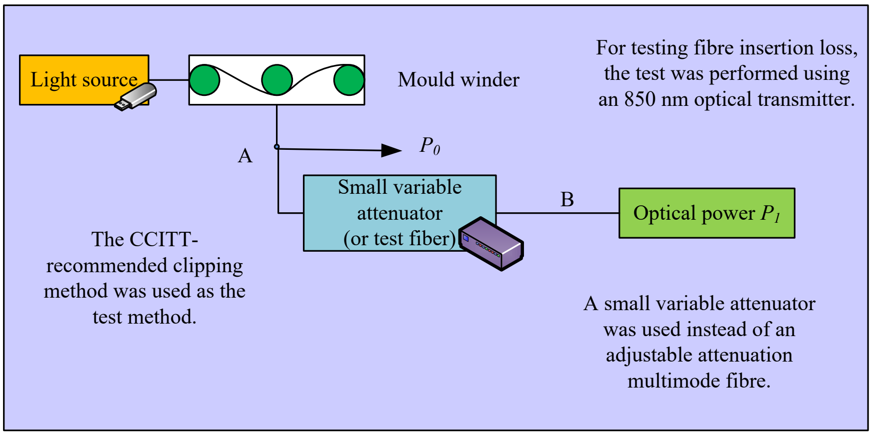

Fig. 5. Fiber loss test block diagram

$$A = 101g(P_3 / P_4) \tag{15}$$

In Equation (15), P_3 is the fiber untwisted measured power. A is the bending loss and P_4 is the power after winding. The study first needs to obtain the optical power number output data, obtain the optical power at different wavelengths by two methods, and then find the relative loss rate. Fig. 6 shows the scrambler winding method.

3. RESULTS

In order to validate the proposed performance testing and optimization method of FOC based on multiple environmental parameters, an experiment is carried out. The objective of this experiment is to validate the method, analyze the corresponding design parameters and experimental data results, validate the advantages and feasibility of the method, and provide a reference for the subsequent monitoring of the FOC lines.

3.1. Experimental results of fiber optic cable grating monitoring in power systems

A vertical stress of 1N applied at the free end is investigated in relation to the practical application. The thickness of its selected cantilever beam is 2 mm and then simulated by Solidworks software. Table 1 shows the simulation results. The strain has reached the desired strain value for the cantilever beam arm length of 10 cm. Although, the longer the cantilever beam, the higher the maximum strain value in the case of constant stress at the free end of the cantilever beam. However, the energy loss of the interaction between the two parts must also be taken into account, and therefore a cantilever beam arm length of 12 cm is selected for the study synthesis.

Table 1. Mechanical simulation results of cantilever beam based on fiber optic grating

Cantilever arm length/mm	Free end displacement of cantilever beam/mm	Maximum strain value/10-5
80	0.256	6.834
100	0.501	9.354
120	0.889	11.365
140	2.842	28.63

Experiments in FOC structure monitoring is pasted two different wavelengths of FG strain gages, set up the name of B1, B2, model 3100. In this study, temperature control experiments will be carried out on the strain gages on the cantilever beams. The temperature fluctuation is shown in Fig. 7. The experimental environment is no-load state and the temperature is in the interval of 0°C-60°C. Fig. 7(c) shows the final calculated temperature compensation effect. In terms of strain wavelength, the maximum temperature-induced wavelength fluctuation deviation is 1 nm. The temperature offset-induced error is within 0.015 nm, and the maximum error is 1.5%, which is within the acceptable range. Fig. 8 reflects the effect of FO grating test. The experiment is the result of long-term operation, testing and

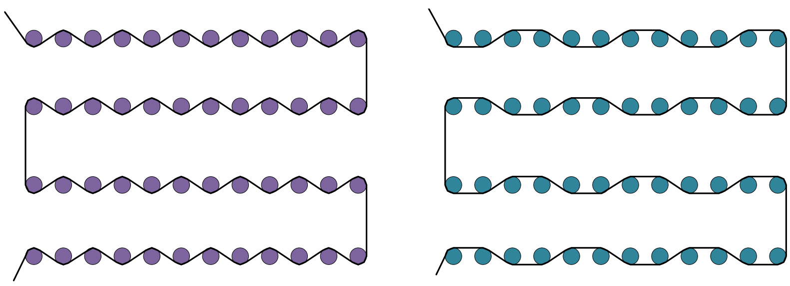

(a) Bending radius R_1 winding method (b) Bending radius R_2 winding method

Fig. 6. Two different winding methods for disturbance models

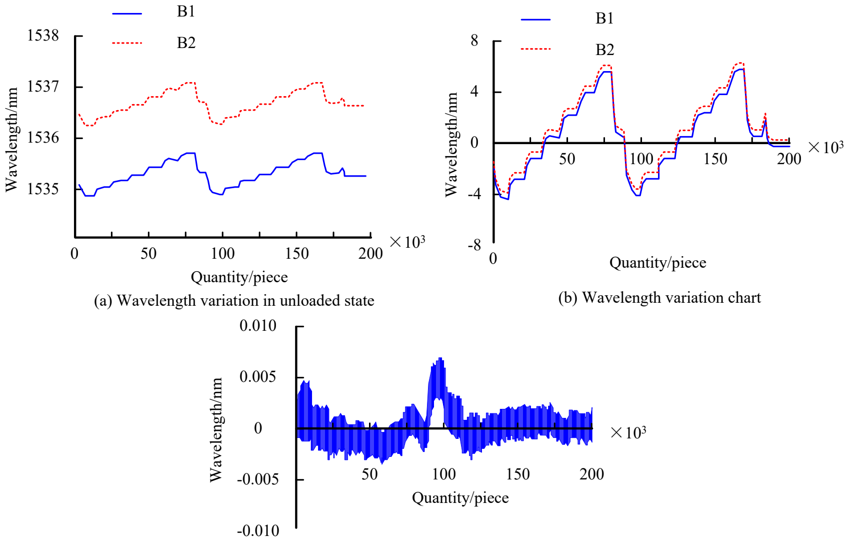

(a) Wavelength variation in unloaded state
(b) Wavelength variation chart
(c) Warm compensation effect diagram

Fig. 7. Performance of dual grating temperature compensation structure

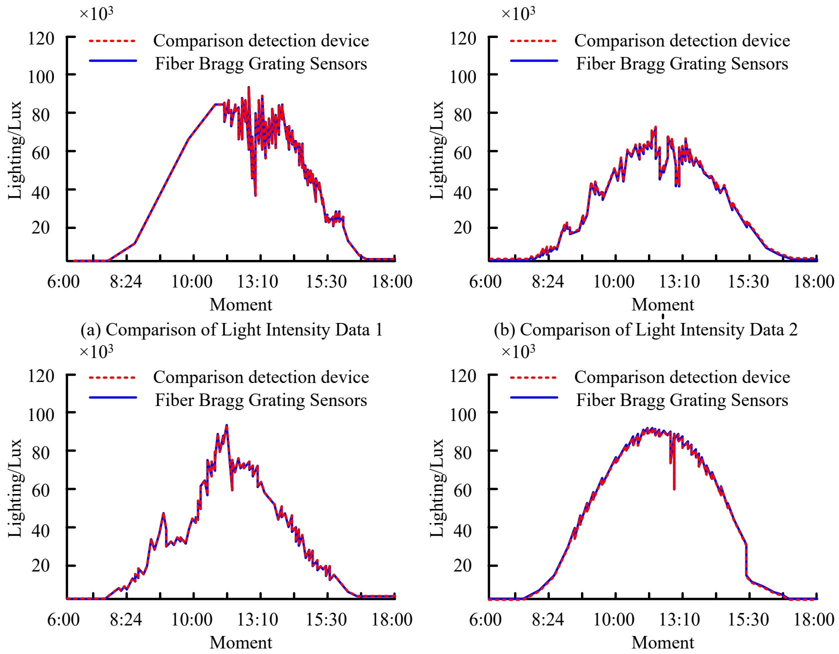

(a) Comparison of Light Intensity Data 1
(b) Comparison of Light Intensity Data 2
(c) Comparison of Light Intensity Data 3
(d) Comparison of Light Intensity Data 4

Fig. 8. Comparison between fiber Bragg grating light monitoring sensors and comparative detection devices

practical application, so the monitoring effect of fiber Bragg grating light monitoring sensor can effectively reflect the actual FOC line loss and other conditions. Moreover, the error of the sensor monitoring results is within 6%. Therefore, the proposed fiber Bragg grating light monitoring sensor can reliably monitor FOC lines.

3.2. Measurement and analysis of fiber optic cable outer layer broken strands with high precision monitoring and loss results

Table 2 illustrates the outcomes of the SNR assessment, which demonstrates that the methodology for signal acquisition proposed by the research's sensor exhibits a high degree of monitoring precision and is capable of retrieving a wealth of valuable insights. This is primarily evident in the acquisition of signals with a notable SNR, reaching up to 57 dB. The processing effect of signal processing can be reflected by the response frequency. With the increase of external signal frequency, the maximum response frequency of the sensor is as high as 6233 and 6315 times/sec, which shows that the method can realize the sensitive response to the corresponding signals on two kinds of FOC.

Fig. 9 presents a comparative analysis of the bending loss associated with the two distinct winding methodologies. For a given state and type of FO, the loss degree varies depending on the wavelength of light signals traversing it. This is due to the differing bending radii of the fibers, which affect the degree of light loss. When considering the same wavelength of optical signal, the loss of B is less than that of A. This is due to the smaller bending radius of A, which results in a larger bending radius for fiber B. It can be observed that adjusting the bending radius can effectively control the degree of loss of the FO. Therefore, compared with 1550nm, the loss of single-mode fiber G.6521 at 1310nm is much lower than that of multi-mode fiber.

To further compare the optimized method of performance detection of FOC proposed in the study, it is compared with the method of accurate measurement of crack width (set up as a comparison method) using a more sensitive fiber cable and a cable with reduced sensitivity but better survivability, as proposed by Liu H et al. Fig. 10(a) shows the detection of different FOC damage

conditions based on temperature parameters by the research method. Among the monitoring information of different FOC sensors, the temperature information can be a good early warning of the FOC condition. One of the FOC 1 sensors 5 has the risk of breaking strands of the outer fuse of the FOC due to lightning strikes. This is mainly manifested in the fact that the location of the temperature change of the FOC 1 sensor 5 is the same as the simulated location of the measured lightning strike. This is shown by the rapid increase in temperature in the first period which in turn leads to an increase in temperature of the FOC in the later period. This clearly demonstrates the accuracy and effectiveness of the proposed method in monitoring high temperature melt strand breakage of FOC.

The temperature change of cable 2 is mainly characterized by the increasing temperature from the sensor 2 and the temperature rise of the 3rd sensor has already reached more than 280°C. Field testing reveals that the cable line at this location is broken, which effectively demonstrates the effectiveness and accuracy of the proposed method in detecting damage to the cable line due to temperature rise and breakage. Field tests reveal that strand breakage at this location is indeed caused by construction stress or fatigue short circuit current temperature rise. This is primarily indicated by the sensor 2 on FOC 2,

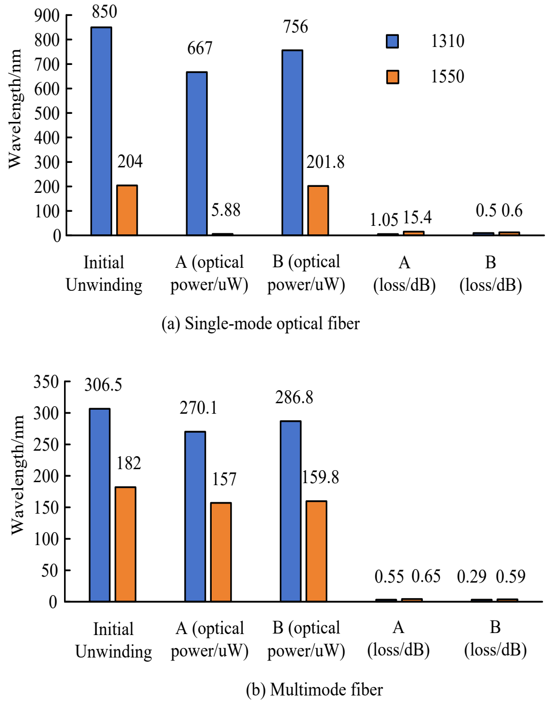

Fig. 9. Comparison of bending losses between two winding methods

whose temperature trend began to rise consistently in the early part of the period. In addition, when monitoring the sensor 3, it is found that its temperature has risen to over 279°C. Fig. 10(b) shows the comparison between the research method and the comparison method for the detection of FOC. The research method is more similar to the actual measurement of the FOC than the comparison method, so the proposed method shows better detection performance.

Table 2. Signal-to-noise ratio test and response frequency test results

Sensor number	External signal frequency/times/s	Signal-to-noise ratio/dB		Sensor maximum response frequency/times/s	
		a	b	a	b
1	6000	125	136	6230	6310
2	5620	136	152	5752	5692
3	6230	152	163	6258	6420
4	5820	142	142	5870	5890
5	5480	136	152	5569	5563
6	5660	128	157	5690	5678
7	4960	136	136	5201	5129
8	4880	152	132	4986	5028
9	5260	142	152	5362	5320
10	5280	153	162	5365	5374

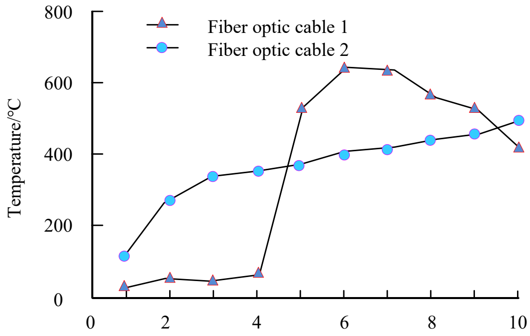

(a) Temperature test results of two experimental optical cables

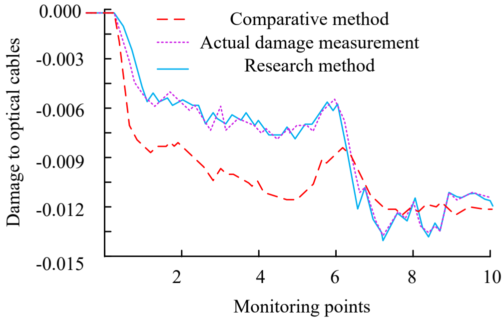

(b) Two methods for detecting accuracy

Fig. 10. Research methods for verifying the performance of fiber optic cables

4. DISCUSSION AND CONCLUSION

In order to achieve the normal operation of FO communication and effective maintenance in the later stage, the study proposes a method for monitoring broken strands in the outer layer of FOCs. This method employed temperature sensing in order to achieve the real-time display of the FO temperature sensor monitoring signals, as well as the study of the SNR and response frequency of the larger sensor signals. The goal of this study was to provide insights for the application and analysis of FOCs. To optimize the monitoring method of FOC performance, a parameter measurement loss analysis based on FO coupling efficiency and NA was introduced. The results indicated that the maximum temperature-induced wavelength fluctuation deviation was 1 nm in terms of strain wavelength. The maximum error of temperature offset was 1.5%, and the error was within 0.015 nm, which was within the acceptable range. The proposed method of the study was able to acquire a large amount of useful information with high monitoring accuracy. The maximum signal acquired by the sensor was around 157 dB, which was able to achieve a high SNR. In addition, the maximum response frequency of the sensor was as high as 6233 and 6315 times/sec with the increase of the external signal frequency, which indicated that the method was able to achieve a sensitive response to the corresponding signals on the two types of FOCs. It can be concluded that the proposed method of the study can obtain high monitoring accuracy, which is of some significance for FO communication and reduction of fiber optic communication loss. However, the study is relatively complicated for the design and installation of FG sensor, so the installation and design of FG sensor need to be further simplified in the subsequent research.

Source of funding: *The research is supported by the Science and Technology Project of State Grid Shanxi Electric Power Company (52051C230002).*

Author contributions: *Research concept and design, J.W., X.D.; Collection and/or assembly of data, H.X., C.H.; Data analysis and interpretation, X.H., J.M.; Writing the article, J.Z.; Critical revision of the article, J.Z., Y.L.; Final approval of the article, Y.L., X.H.*

Declaration of competing interest: *The author declares no conflict of interest.*

REFERENCES

1. Yan Y, Zheng H, Zhao Z, Guo C, Wu X, Hu J, Lu C. Distributed optical fiber sensing assited by optical communication techniques. Journal of Lightwave Technology. 2021;39(12):3654-3670. http://doi.org/10.1109/JLT.2021.3057670.
2. Wang Z, Shen Z, Wang Z, Zhang J, Zhao J, Wan H. High accuracy, multi-signal demodulation method for distributed, wide-frequency domain optical fiber sensing. Optical Fiber Technology. 2022;70(5):1-6. https://doi.org/10.1016/j.yofte.2022.102850.
3. Lyu C, Hu X, Niu Z, Yang B, Jin J, Ge C. A light-weight neural network for marine acoustic signal recognition suitable for fiber-optic hydrophones. Expert Systems with Application. 2024;235(1): 121235.1-121235.9. https://doi.org/10.1016/j.eswa.2023.121235.
4. Gutierrez F, Sevil J, Sevillano P, Preciado-Garbayo J, Martinez JJ, Martin-Lopez S. The application of distributed optical fiber sensors (BOTDA) to sinkhole monitoring. Review and the case of a damaging sinkhole in the Ebro Valley evaporite karst (NE Spain). Engineering Geology. 2023;325(13):107289-107291. https://doi.org/10.1016/j.enggeo.2023.107289.
5. Liu Z, Wang Y, Chen X, Meng X, Liu X, Yao J. An optical fiber sensing method for partial discharge in the HVDC cable system. International Journal of Electrical Power & Energy Systems. 2021;128(2): 106749.1-106749.9. https://doi.org/10.1016/j.ijepes.2020.106749.
6. Zhou F, Duan W, Li X, Tsai J, Jun MBG. High precision in-situ monitoring of electrochemical machining process using an optical fiber Fabry-Pérot interferometer sensor. Journal of Manufacturing Processes. 2021;68(9):180-188. https://doi.org/10.1016/j.jmapro.2021.07.010.
7. Liu H, Zhang S, Coulibaly AAS, Cheng J, Dejong MJ. Monitoring reinforced concrete cracking behavior under uniaxial tension using distributed fiber-optic sensing technology. Journal of Structural Engineering. 2021;147(12): 4021212.1-4021212.19.

https://doi.org/10.1061/(ASCE)ST.1943-541X.0003191.

8. Hao Y, Chen Y, Chen Y, Huang T, Xiao J, Yang L. A partial discharge detection system for XLPE cable terminals and acoustic wave sensing characteristics based on fiber optic mach-zehnder interferometer. IEEE Sensors Journal. 2021;21(19):21782-21790. https://doi.org/10.1109/jsen.2021.3101835.
9. Hou GY, Li ZX, Wang KD, Hu JX. Structural deformation sensing based on distributed optical fiber monitoring technology and neural network. KSCE Journal of Civil Engineering. 2021;25(11):4304-4313. https://doi.org/10.1007/s12205-021-1805-z
10. Zhang S, Liu H, Coulibaly AAS, Matthew D. Fiber optic sensing of concrete cracking and rebar deformation using several types of cable. Structural Control and Health Monitoring. 2020;28(2):e2664.1-e2664.23. https://doi.org/10.1002/stc.2664
11. Huang S, Hu X, Zhang H, Chen W, Huang Y, Fan M. A high-precision system of fiber Bragg grating temperature sensing demodulation based on light power detection. Optoelectronics Letters. 2022;18(8): 461-467.https://doi.org/10.1007/s11801-022-2025-6
12. Lin W, Huang Y, Li Z. ZIF-90-derived porous ZnO coated optical microfiber interferometer sensor for enhanced humidity sensing and breath monitoring. ACS Applied Materials & Interfaces. 2023;15(26): 32057-32065. https://doi.org/10.1021/acsami.3c06635.
13. Shao T, Liu Z. Design of pulse and respiration monitoring system based on fiber optic sensing and VMD-FPR processing algorithm. Optical Fiber Technology. 2022;73(10):103033.1-103033.10. https://doi.org/10.1016/j.yofte.2022.103033.
14. Zhao S, Liu Q, Liu Y, He Z. Femto-strain resolution fiber-optic sensing with an ultra-simple white-light round trip filtering method. Optics Letters. 2022; 47(15):3624-3627. https://doi.org/10.1364/OL.463204.
15. Rente B, Fabian M, Vidakovic M, Vorreiter L, Grattan KTV. Extended study of fiber optic-based humidity sensing system performance for sewer network condition monitoring. IEEE Sensors Journal. 2021; 21(6):7665-7671. https://doi.org/10.1109/JSEN.2021.3050341.
16. Okamoto T, Iida D, Koshikiya Y, Honda N. Deployment condition visualization of aerial optical fiber cable by distributed vibration sensing based on optical frequency domain reflectometry. Journal of Lightwave Technology. 2021;39(21):6942-6951. https://doi.org/10.1109/JLT.2021.3107855.
17. Zolfaghari P, Erden OK, Ferhanoglu O, Tumer M, Yalcinkaya AD. MRI compatible fiber optic multi sensor platform for real time vital monitoring. Journal of Lightwave Technology. 2021;39(12):4138-4144. https://doi.org/10.1109/JLT.2021.3055252.
18. Sun Y, Xue Z, Park H, Hashimoto T, Zhang Y. Optical sensing of CO2 geological storage using distributed fiber-optic sensor: From laboratory to field-scale demonstrations. Energy & Fuels. 2020;35(1):659-669. https://doi.org/10.1021/acs.energyfuels.0c03925.
19. Li ZX, Hou GY, Hu T, Zhou T, Xiao HL. A study on the application of the distributed optical fiber sensing monitoring technology in the process of dismantling temporary tunnel shoring. Arabian Journal of Geosciences. 2020;13(19):1-11. https://doi.org/10.1007/s12517-020-06069-0.
20. Bandewad G, Datta KP, Gawali BW, Pawar SN. Review on discrimination of hazardous gases by smart sensing technology. Artificial Intelligence and Applications. 2023;1(2):86-97. https://doi.org/10.47852/bonviewAIA3202434.

Jianliang ZHANG, born in June 1981, male, from Wutai, Shanxi, Han ethnicity. He obtained a Bachelor's degree in Electronic Science and Technology from Jilin University in 2004 and a Master's degree in Electronic and Communication Engineering from Taiyuan University of Technology in 2013, with a research focus on power communication.

Work experience: From 2006 to 2012, worked as a communication operation and maintenance specialist at Shanxi Electric Power Communication Center; From 2013 to 2022, worked as a technology management specialist at the State Grid Information & Telecommunication CO. of Shanxi Electric Power Company; From 2023 to present, worked as a material management specialist at the State Grid Information & Telecommunication CO. of Shanxi Electric Power Company.

Academic situation: Led or participated in 14 scientific and technological projects undertaken by Shanxi Province, State Grid Corporation of China, and provincial companies; Published 1 book, 6 papers in Chinese core journals, 9 papers indexed by EI, and 8 authorized invention patents; Received one second prize for scientific and technological progress in Shanxi Province and six other provincial and ministerial level innovative achievements.

e-mail: sxdlzjl@163.com

Yang LI, born in April 1978, male, from Laizhou City, Shandong Province, Han ethnicity. He obtained his PhD in Mechanical Design and Theory from Harbin Institute of Technology in November 2008. In March 2011, postdoctoral fellow at Inspur Group and Shandong University, with a research focus on data mining.

Work experience: From 2011 to 2012, worked as a pre planning specialist in the System Management Department of Shanxi Electric Power Communication Center. From 2012 to this year, worked as a fourth level employee in the Technology Development Department of the State Grid Information & Telecommunication CO. of Shanxi Electric Power Company.

Academic situation: Published more than 10 articles indexed in EI and SCI, authorized more than 20 patents, completed more than 10 scientific and technological projects, and won two Shanxi Provincial Science and Technology Progress Awards.

e-mail: ansysman@126.com

Xiaowei HAO, born in September 1982, male, from Yuncheng, Shanxi, Han ethnicity. He obtained a Bachelor's degree in Electronic Information Engineering from North China Electric Power University in 2004 and a Master's degree in Electronic and Communication Engineering from

Taiyuan University of Technology in 2008, with a focus on power communication.
Work experience: Since 2017, he has been working as a team leader at the State Grid Information & Telecommunication CO. of Shanxi Electric Power Company.
Academic situation: Published 3 papers including Chinese core papers; Authorized 3 invention patents.
e-mail: haoxiaowei@sx.sgcc.com.cn

Junwei MA, born in September 1982, male, from Jining, Shandong, Han ethnicity. He obtained a Bachelor's degree in Applied Mathematics from Yantai University in 2005, a Master's degree in Basic Mathematics from Dalian University of Technology in 2007, and a PhD in Control Theory and Control Engineering from Dalian University of Technology in 2011. His research focuses mainly on power big data and artificial intelligence applications.
Work experience: From 2011 to 2012, worked as a system maintenance specialist in the Network Department of the Power Communication Center at State Grid Shanxi Electric Power Company; From 2012 to 2017, under the comprehensive planning management of the Technology Development Department of the State Grid Information & Telecommunication CO. of Shanxi Electric Power Company; From 2017 to 2020, Assistant Manager of the Grid Technology Branch of Jindian Electric Power Technology Co., Ltd; From 2020 to 2024, served as the Deputy Director of the Technology Development Department at the State Grid Information & Telecommunication CO. of Shanxi Electric Power Company; 2024 present, Level 4 Technology Expert at the Big Data Center of State Grid Information & Telecommunication CO. of Shanxi Electric Power Company.
Academic situation: Hosted more than 10 projects of Shanxi Provincial Department of Science and Technology, State Grid, and Shanxi Electric Power Technology, published more than 20 papers, authorized more than 10 patents, published 3 books, obtained national and international advanced certification certificates such as PMP, CISP, ITIL, etc., served as the secretary of the Access Network Group of the Power Communication Special Committee of the China Electrical Engineering Society for two consecutive terms, and is currently a member of the China Energy Research Association, the China Automation Society, and the China Computer Society. He has won the honorary titles of "Three Jin Talents" in Shanxi Province, senior expert in information and communication of State Grid Corporation, silver medal of Youth Innovation Competition of State Grid Corporation, model worker of State Grid Shanxi Electric Power Company, etc.
e-mail: junweima@foxmail.com

Honglin XUE, born in July 1981, male, from Wanrong, Shanxi, Han ethnicity, obtained a Bachelor's degree in Electronic Information Engineering from Shanxi University in 2004 and a Master's degree in Electronic and Communication Engineering from North China Electric Power University in 2013, with a research focus on power communication.
Work experience: From 2003 to 2010, worked as a communication operation and maintenance manager at Shanxi Electric Power Communication Center; From 2011 to 2012, worked as the deputy director of the network department at Shanxi Electric Power Communication Center; From 2013 to 2019, worked as the director of the control center at the State Grid Information & Telecommunication CO. of Shanxi Electric Power Company; From 2019 to 2023, worked as the director of the Technology Development Department at the State Grid Information & Telecommunication CO. of Shanxi Electric Power Company; From 2023 to present, worked as the deputy general manager of the State Grid Information & Telecommunication CO. of Shanxi Electric Power Company.
Academic situation: Undertook 6 scientific and technological projects for Shanxi Province, State Grid Corporation of China, and provincial companies; Published 3 papers in Chinese core journals, 9 papers indexed by EI, and granted 4 invention patents; Received one second prize for scientific and technological progress in Shanxi Province.
e-mail: xuehonglin@sx.sgcc.com.cn

Chao HAN, born in July 1985, male, native of Wuxiang County, Shanxi Province, Han ethnicity, obtained a Bachelor's degree in Electrical Engineering and Automation from Xihua University in 2008, with a research focus on Information and Communication.
Work experience: Employee of State Grid Shanxi Jinzhong Power Supply Company from 2008 to 2014; Employee of Shanxi Jinyuan Network Technology Co., Ltd. from 2014 to 2017; Employee of State Grid Information & Telecommunication CO. of Shanxi Electric Power Company from 2018 to present.
Academic situation: Undertook 4 science and technology projects for State Grid Corporation of China and provincial companies; Published 5 papers and obtained 2 authorized invention patents.
e-mail: feelingandy@hotmail.com

Jian WU, born in February 1990, male, from Xiangfen, Shanxi, Han ethnicity. He obtained a Bachelor's degree in Communication Engineering from the University of Electronic Science and Technology of China in 2012 and a Master's degree in Communication and Information Systems from the University of Electronic Science and Technology of China in 2015. His main research direction is related to the planning and construction of power communication systems.
Work experience: From 2015 to 2018, he was responsible for the operation and inspection center of the State Grid Information & Telecommunication CO. of Shanxi Electric Power Company; From 2018 to 2019, he served as the team leader of the operation and inspection center of the State Grid Information & Telecommunication CO. of Shanxi Electric Power Company; From 2019 to present, he has been responsible for communication planning and management in the Technology Development Department of the State Grid Information & Telecommunication CO. of Shanxi Electric Power Company.
Academic situation: Published 4 core Chinese papers such as "Intelligent Recognition of Fiber Optic Links Based on

Physical Address Encoding", authorized 6 invention patents, undertaken key research projects of State Grid Shanxi Electric Power Company multiple times, won multiple awards such as the first prize for scientific and technological progress of the provincial company, and was awarded as an excellent engineer in Shanxi's power industry during the 13th Five Year Plan period.
e-mail: soianjoker@gmail.com

Xiaoyan DANG, born on July 11, 1987, female, from Xinzhou, Shanxi, Han, obtained a Bachelor's degree in Electrical Engineering and Automation from Nanjing University of Science and Technology in 2009.
Work experience: From 2009 to 2014, worked at the Information and Communication Department of State Grid Xinzhou Power Supply Company; From 2014 to 2017, worked at the Information Technology Department of Shanxi Jinyuan Network Technology Co., Ltd; From 2017 to present, worked at the Technology Development Department of State Grid Information & Telecommunication CO. of Shanxi Electric Power Company.
Academic situation: Undertook 6 science and technology projects for State Grid Corporation of China and provincial companies; Published 5 papers and obtained 2 authorized invention patents.
e-mail: dxy2488@163.com